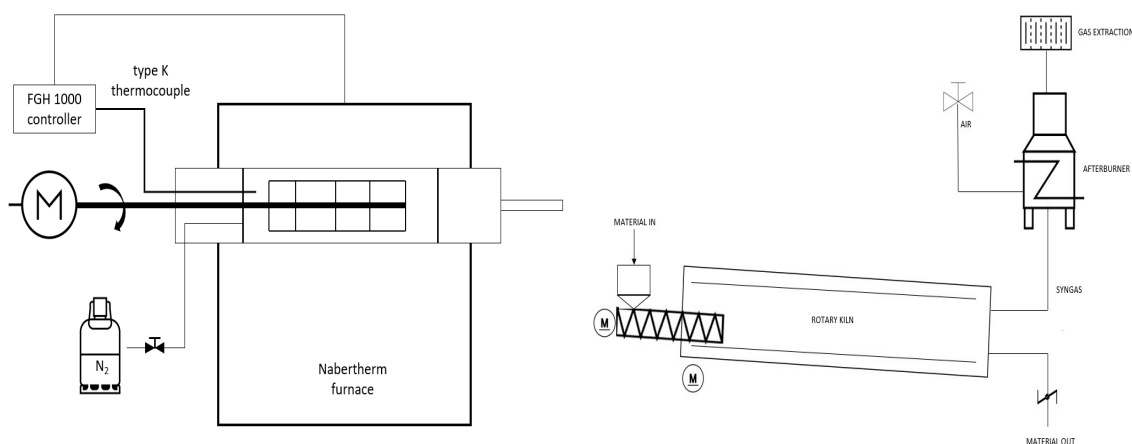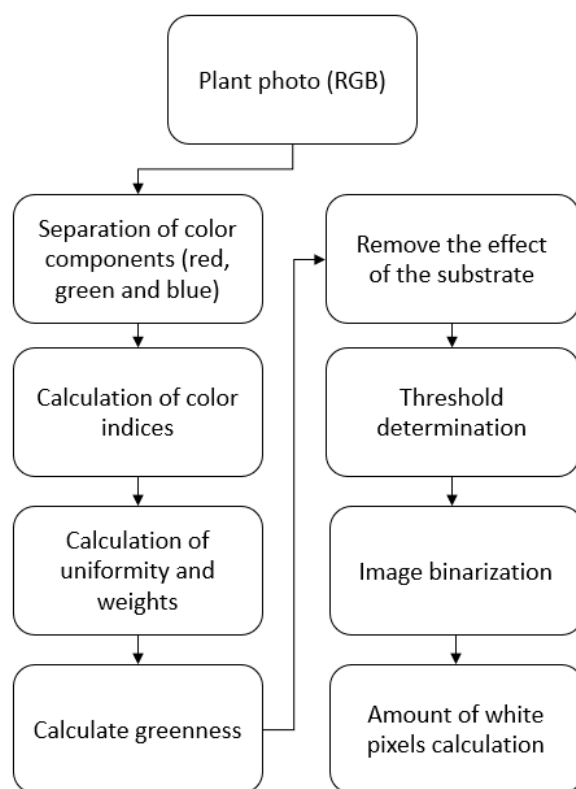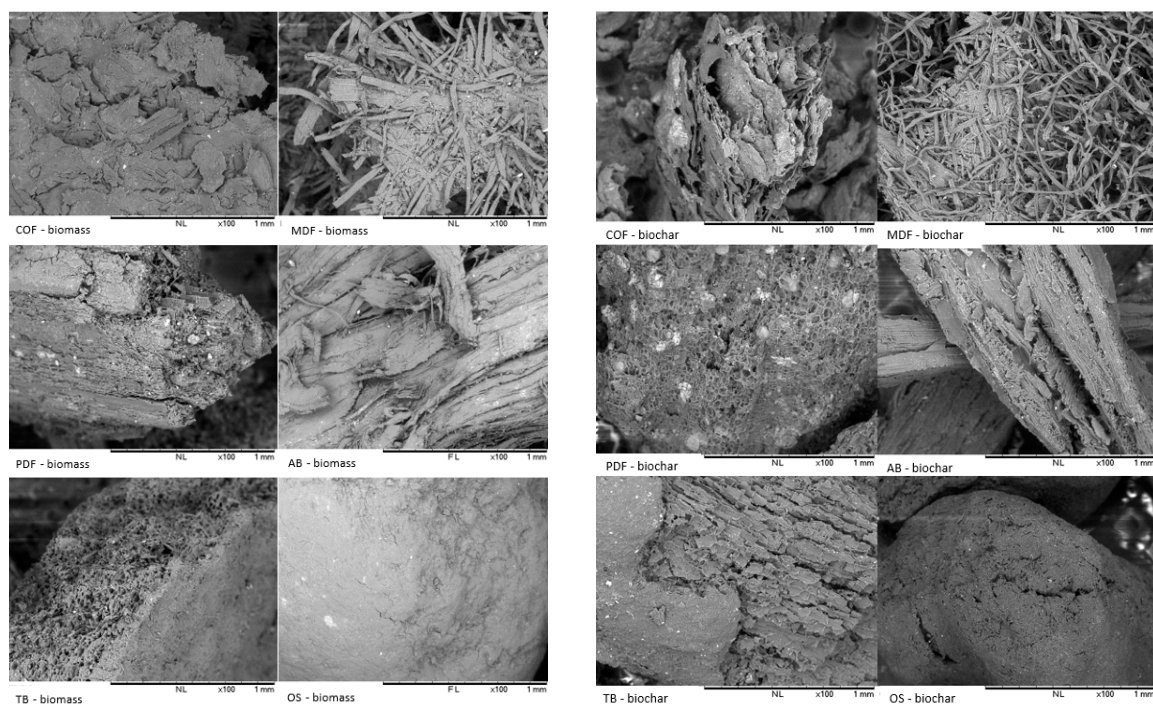# An Experimentally Validated Selection Protocol for Biochar as a Sustainable Component in Green Roofs
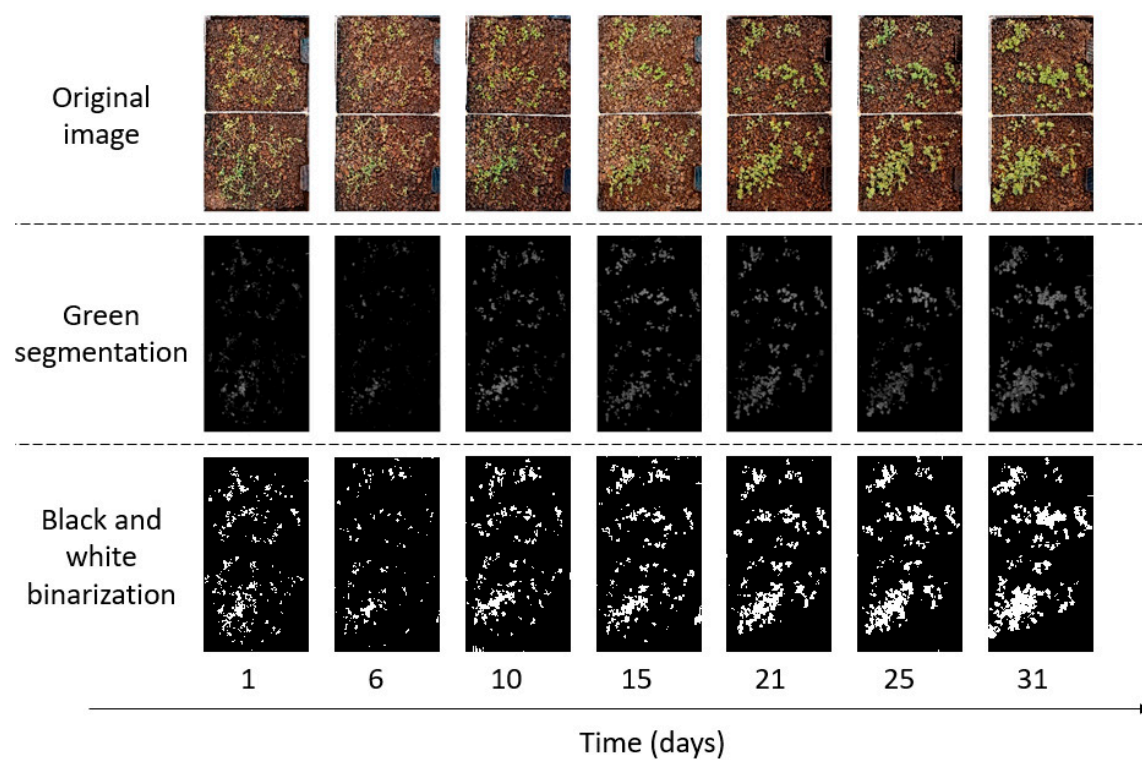

Figure S1. Schematic representation of the lab-scale batch reactor (left) and the pilot scale reactor (right) [1].

Figure S2. Flow diagram for green segmentation strategy.

Figure S3. SEM images of biomasses and biochars produced in the pilot scale reactor (T = 450 °C).

Figure S4. Growth process of Sedum Hispanicum approached as surface green coverage on substrate with 5 wt. % of biochar during 31 days. Top: original image, middle: image after green segmentation and bottom: image after black and white binarization.

Table S1. Band assignments of FT-IR spectra of the different biomass samples. Results of FT-IR for MDF were previously published [2].

Wavenumber (cm^{-1})	COF	MDF	PDF	AB	TB	OS	Peak shape	Band assignment	Source
3600-3100	x	x	x	x	x	x	Very broad	Multitude of OH stretching in the phenolic and aliphatic structures of cellulose, hemicellulose and lignin. When N is present in higher concentrations (COF, MDF and AB), NH stretching vibrations are also found.	[3]
2950,2925 and 2850	x	x	x	x	x	x	Shoulder + sharp double peak	Symmetric and asymmetric C-H stretching vibrations	[3, 4]
1736	x	x	x	x	x	x	Broad	C=O stretch hemicellulose	[4]
1643	x	x	x	x	x	x	Broad	OH-bending of absorbed water	[5]
1608	x	x	x	x	x	x	Broad	C=C symmetric stretching of aromatic ring systems	
1539	x	x		x		x	Weak	C=C stretch in a nitrogen based ring	[6]
1513	x	x	x	x	x	x	Weak	Aromatic ring vibration in lignin	[5]
1455	x	x	x	x	x	x	Weak	CH$_3$ and CH$_2$ deformation	[3, 5]
1425	x	x	x	x	x	x	Weak	HCH and OCH in plane bending vibration of cellulose	[3]
1371	x	x	x	x	x	x	Weak	CH and OH bending	[3]
1321	x	x	x	x	x	x	Weak	CH$_2$ wagging in cellulose and hemicellulose or OH bending	[3]
1262	x	x		x	x		Sharp	aromatic ring vibration of guaiacyl lignin	[3]
1240	x	x	x	x	x	x	Broad	C-O stretch and O-H in plane bending in polysaccharides and syringyl lignin	[4]
1155	x	x	x	x	x	x	Shoulder	C-O-C band vibration in cellulose and hemicellulose	[3, 5]
1106	x	x	x	x	x	x	shoulder	O-H band vibration in cellulose and hemicellulose	[3, 5]
1050	x	x	x	x	x		Shoulder	C-O stretching in holocellulose	[7]
1033	x	x	x	x	x	x	Very sharp	aromatic C-H in plane deformation of guaiacyl lignin and C-O deformation	[3–5]
893	x	x	x	x	x	x	Weak	COC, CCO and CH deformation in cellulose and hemicellulose	[5]
808	x	x	x	x	x	x	Weak	C-H bending	
772	x	x	x	x	x	x	Weak	C-H bending	
718	x	x	x	x			Weak	Ca-O bonds	[8]

Table S2. Band assignments of FT-IR spectra of the different biochar samples, adapted from [2, 9–12]. Results of FT-IR for MDF were previously published [2].

Wavenumber (cm^{-1})	COF	MDF	PDF	AB	TB	OS	Trend with increasing temperature	Band assignment
3600-3100	x	X	x	x	x		--	Multitude of OH-stretching frequencies in phenolic and aliphatic structures of degradation products of cellulose, hemicellulose and lignin or N-H stretching in biomasses with enhanced N content
3025		X	x				++	C_{sp2}-H stretching vibration of aromatic structures
2950,2925 and 2850	x	X	x	x		x	--	C-H symmetric and asymmetric bond stretching in aliphatic and alicyclic components
2175	x						++	Nitrile groups
1700-1600	x	x	x	x		x	--	C=O stretching vibrations as found in degradation products of hemicellulose
1580		x	x	x	x	x	Normalized	C=O stretching of aromatic moieties
1435		x					++	C=C stretching of aromatic moieties
1420	x		x		x		++	CaCO$_3$ and other carbonates like K$_2$CO$_3$
1375		x		x			--	C-H deformation
1300-1100	x					x	--	C-N and C-O functionalities
1160			x		x	x	--	C-O stretching
1107			x				++	Si-O bonds*
1020		x		x		x	++	Aromatic ethers
875 (High ash biomass)	x		x		x		++	CaCO$_3$ and other carbonates like K$_2$CO$_3$
875 (Low ash biomass)		x		x		x	++	Aromatic C-H bending
810		x		x	x	x	++	Aromatic C-H bending
755		x	x	x	x	x	++	Aromatic C-H bending
718	x		x		x		++	CaCO$_3$ and other carbonates like K$_2$CO$_3$
675		x	x	x	x	x	++	Aromatic C-H out of plane bending
620	x	x	x		x		++	Aromatic C-H out of plane bending

Table S3. Heavy metal concentrations in all biochars.

	As (mg/kg)	Cd (mg/kg)	Cr (mg/kg)	Cu (mg/kg)	Hg (mg/kg)	Ni (mg/kg)	Pb (mg/kg)	Zn (mg/kg)
COF350	<100	<10	<20	213 ± 12	<100	<20	<100	108 ± 2
COF450B	<100	<10	<20	235 ± 10	<100	<20	<100	108 ± 5
COF500	<100	<10	<20	292 ± 3	<100	<20	<100	122 ± 1
COF550	<100	<10	<20	248 ± 5	<100	<20	<100	110 ± 1
COF450C	<100	<10	<20	195 ± 2	<100	<20	<100	91 ± 2
MDF350	<100	<10	<20	24 ± 1	<100	<20	<100	28 ± 1
MDF450B	<100	<10	<20	19 ± 1	<100	<20	<100	27 ± 1
MDF500	<100	<10	25 ± 2	32 ± 4	<100	<20	<100	52 ± 4
MDF550	<100	<10	<20	50 ± 1	<100	<20	<100	57 ± 4
MDF450C	<100	<10	<20	21 ± 1	<100	<20	<100	<20
PDF350	<100	<10	105 ± 1	<20	<100	121 ± 8	<100	<20
PDF450B	<100	<10	39 ± 6	<20	<100	<20	<100	<20
PDF500	<100	<10	30 ± 1	<20	<100	<20	<100	<20
PDF550	<100	<10	108 ± 5	<20	<100	<20	<100	<20
PDF450C	<100	<10	<20	28 ± 2	<100	<20	<100	69 ± 1
AB350	<100	<10	124 ± 4	87 ± 1	<100	481 ± 11	488 ± 10	485 ± 49
AB450B	<100	<10	135 ± 1	123 ± 7	<100	524 ± 42	534 ± 40	572 ± 36
AB500	<100	<10	135 ± 4	105 ± 1	<100	589 ± 50	599 ± 60	553 ± 25
AB550	<100	<10	155 ± 5	149 ± 11	<100	1372 ± 20	1402 ± 26	976 ± 34
AB450C	<100	<10	141 ± 2	161 ± 8	<100	<20	321 ± 27	315 ± 19
TB350	<100	<10	<20	31 ± 1	<100	<20	<100	159 ± 7
TB450B	<100	<10	<20	27 ± 1	<100	<20	<100	145 ± 4
TB500	<100	<10	24 ± 2	33 ± 7	<100	<20	<100	135 ± 8
TB550	<100	<10	25 ± 3	42 ± 5	<100	<20	<100	130 ± 2
TB450C	<100	<10	<20	29 ± 1	<100	<20	<100	148 ± 3
OS350	<100	<10	<20	26 ± 1	<100	<20	<100	<20
OS450B	<100	<10	<20	25 ± 1	<100	<20	<100	<20
OS500	<100	<10	67 ± 13	29 ± 2	<100	<20	<100	<20
OS550	<100	<10	73 ± 14	50 ± 3	<100	55 ± 1	<100	21 ± 2
OS450C	<100	<10	<20	22 ± 1	<100	<20	<100	<20

References

1. Haeldermans T., Lataf M.A., Vanroelen G., et al. Numerical prediction of the mean residence time of solid materials in a pilot-scale rotary kiln. *Powder Technol.* **2019**, *354*, 392–401. https://doi.org/10.1016/j.powtec.2019.06.008
2. Haeldermans T., Claesen J., Maggen J., et al. Microwave assisted and conventional pyrolysis of MDF – Characterization of the produced biochars. *J. Anal. Appl. Pyrolysis* **2019**, *138*, 218–230. https://doi.org/10.1016/j.jaap.2018.12.027
3. Xu F., Yu J., Tesso T., et al. Qualitative and quantitative analysis of lignocellulosic biomass using infrared techniques: A mini-review. *Appl. Energy* **2013**, *104*, 801–809. https://doi.org/10.1016/j.apenergy.2012.12.019
4. Acquah G.E., Via B.K., Fasina O.O., Eckhardt L.G. Rapid Quantitative Analysis of Forest Biomass Using Fourier Transform Infrared Spectroscopy and Partial Least Squares Regression. *J. Anal. Methods Chem.* **2016**, *2016*, 1–11. https://doi.org/10.1155/2016/1839598
5. Müller G., Bartholme M., Kharazipour A., Polle A. FTIR-ATR spectroscopic analysis of changes in fiber properties during insulating fiberboard manufacture of Beech Wood. *Wood Fiber Sci.* **2008**, *40*, 532–543
6. Lyman D.J., Benck R., Dell S., et al. FTIR-ATR analysis of brewed coffee: Effect of roasting conditions. *J. Agric. Food Chem.* 2003, 51,3268–3272. https://doi.org/10.1021/jf0209793
7. Lao W., Li G., Zhou Q., Qin T. Quantitative analysis of biomass in three types of wood-plastic composites by FTIR spectroscopy. *BioResources* **2014**, *9*, 6073–6086. https://doi.org/10.15376/biores.9.4.6073-6086
8. Galvàn-Ruiz M., Hernàndez J., Baños L., et al. Characterization of Calcium Carbonate, Calcium Oxide, and Calcium Hydroxide as Starting Point to the Improvement of Lime for Their Use in Construction. *J. Mater. Civ. Eng.* **2009**, *21*, 694–698. https://doi.org/10.1061/(ASCE)0899-1561(2009)21:11(694)
9. Liu Y., He Z., Uchimiya M. Comparison of Biochar Formation from Various Agricultural By-Products Using FTIR Spectroscopy. *Mod. Appl. Sci.* **2015**, *9*, 246–253. https://doi.org/10.5539/mas.v9n4p246
10. Zhao L., Cao X., Mašek O., Zimmerman A. 2013 Heterogeneity of biochar properties as a function of feedstock sources and production temperatures. *J. Hazard. Mater.* **2013**, *256*, 1–9. https://doi.org/10.1016/j.jhazmat.2013.04.015
11. Molenda J., Swat M., Osuch-Słomka E. Effect of Thermal Conditions of Pyrolysis Process on the Quality of Biochar Obtained from Vegetable Waste. *Eng. Prot. Environ.* **2018**, *21*, 289–302. https://doi.org/10.17512/ios.2018.3.7
12. Dai L., Tan F., Li H., et al. Calcium-rich biochar from the pyrolysis of crab shell for phosphorus removal. *J. Environ. Manage.* **2017**, *198*, 70–74. https://doi.org/10.1016/j.jenvman.2017.04.057